

2D semiconductor structures as a basis for new high-tech devices (Review)

D.V. Korbutyak¹, V.G. Lytovchenko¹, M.V. Strikha^{1,2}

¹ V. Lashkaryov Institute of Semiconductor Physics, NAS of Ukraine, 41, prospect Nauky, 03028 Kyiv, Ukraine
E-mail: kd45@isp.kiev.ua

² Taras Shevchenko Kyiv National University, Radiophysical Faculty, 4g, prospect Akademika Hlushkova, 03022 Kyiv, Ukraine

Abstract. In this article, we present a short overview of the Ukrainian contribution into physics of 2D semiconductor structures as a basis for high-tech devices of modern nanoelectronics together with some new results in this field. The possibility of creating “low-threshold” 2D lasers in $\text{Si}_3\text{N}_4\text{-GaAs}$ and $\text{Al}_x\text{Ga}_{1-x}\text{As-GaAs}$ layered heterostructures, in which two-dimensional electron-hole plasma (EHP) is formed, has been analyzed. The investigations of optical amplification spectra in heterostructures with a two-dimensional quantum well have been performed in details. It has been demonstrated that under the conditions of simultaneous co-existence of 3D-EHP and 2D-EHP, stimulated radiation is formed predominantly in 2D-EHP, with the laser excitation threshold at which optical amplification occurs in 2D-EHP by two orders of magnitude lower than in 3D-EHP, and the corresponding value of the coefficient of optical amplification is 2.5 times greater. A simple theoretical model of electron heating in a system with two valleys is applied to describe 2D semiconductor monolayers of the MoS_2 and WS_2 types. The model is demonstrated to describe sufficiently well the available experimental data on the negative differential conductance effect in a WS_2 monolayer. It confirms the possibility to fabricate Gunn diodes of a new and advanced EMW generation based on the structures concerned. These diodes are capable to generate frequencies of the order of 10 GHz and higher, which makes them attractive for HF practical applications.

Keywords: 2D semiconductor, electron-hole plasma, optical gain, laser emission, Gunn diode.

doi: <https://doi.org/10.15407/spqeo21.04.380>

PACS 42.55.Px, 78.55.-m, 78.60.-b, 78.67.-n, 85.30.Fg, 85.35.Be

Manuscript received 01.11.18; revised version received 23.11.18; accepted for publication 29.11.18; published online 03.12.18.

1. Surface electron-hole plasma for designing 2D lasers

2D lasers that are characterized by an ultralow power (several orders of magnitude lower than that for the 3D lasers with laser excitation) have become, in recent years, one of the central areas of laser physics and engineering. The basic problem here is formation of a photosensitive material monolayer (*e.g.*, SeS_2 , WS_2 , MoS_2 and some other layered semiconductors), in which stimulated radiation is obtained and which is placed in an optical resonator with a terminal output of laser radiation [1, 2].

Much earlier than current publications, the stimulated radiation of 2D electron-hole plasma (2D-EHP) was observed and analyzed in the Department of Surface Science, V. Lashkaryov Institute of

Semiconductor Physics, NAS of Ukraine by V.G. Lytovchenko and D.V. Korbutyak *et al.* [3-8].

By contrast to the monolayer design, where the existence of stimulated emission requires the use of ultrahigh technologies (atomic molecular, MBE deposition *etc.*), the proposed method involves condensation of excitons at the surface and then formation of quasi-2D plasma due to various mechanisms: surface traps, attraction mirror image forces, narrowing the energy gap near the surface at high concentrations of excited charge carriers, creation of a surface potential well for excitons, *etc.* Consequently, a liquid 2D electron-hole phase (EHP) of high density can be obtained at the surface, which, in the presence of intense excitation, causes stimulated radiation, and in the presence of a resonator, can form a laser beam.

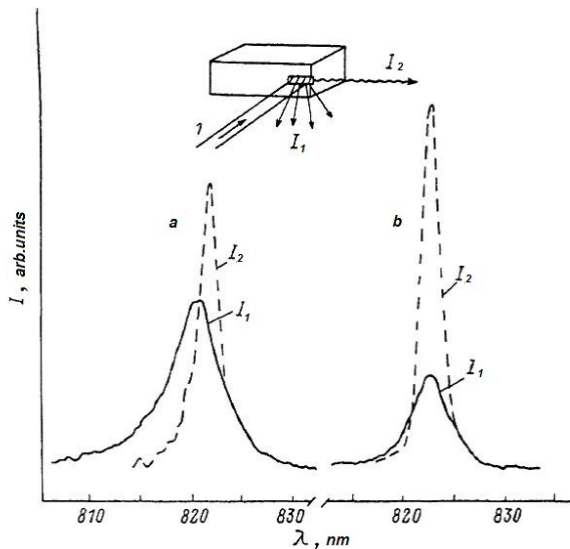


Fig. 1. Spontaneous (I_1) and stimulated (I_2) emission spectra of GaAs (a) and interface Si_3N_4 -GaAs (b) at 4.2 K; the excitation density $L = 5.5 \text{ MW/cm}^2$.

The process of condensed EHP formation at Si_3N_4 -GaAs [3, 4] interfaces and at ion-bombarded ZnO [5, 6] surface was studied earlier in details. The main peculiarities of a 2D electron-hole condensate (2D-EHC) in comparison to those of a three-dimensional (3D) one were analyzed. A number of important peculiarities are to be expected also for stimulated radiation of 2D-EHP [6-8]. Below, we shall describe new data concerning properties of the non-equilibrium 2D-EHP and perspectives for new 2D laser devices.

Let us analyze the spectra of spontaneous and stimulated emission in Si_3N_4 -GaAs and GaAs- $\text{Al}_x\text{Ga}_{1-x}\text{As}$ heterostructures over a wide range of excitation intensities and compare the thresholds at which optical gain first appears for the quasi-2D- and 3D-EHP. On the base on our analysis of the shape of the optical gain spectrum, we then determine the fundamental parameters of EHP formed at extremely high excitation levels. By taking into account outward streaming effects, we can determine the kinetic (drift) characteristics of the 2D plasma and compare it with the 3D case.

In order to investigate the photoluminescence (PL) spectra, we used a LGN-502 CW argon laser and a pulsed Nd^{3+} :YAG laser (the second harmonic of the latter). We used also a MDR-23 monochromator to record the emission spectra, and we got the spectra of the optical gain coefficients (according to the method described in [6]). Fig. 1 demonstrates spontaneous and stimulated bulk (3D) emission spectra of GaAs and interface Si_3N_4 -GaAs, and Fig. 2 presents a comparison of the spontaneous and stimulated emission spectra of the GaAs- $\text{Al}_{0.3}\text{Ga}_{0.7}\text{As}$ heterostructures under pulsed laser excitation at various power densities. For the excitation levels used, we observed two bands in the spontaneous emission spectrum, one due to irradiative recombination of electrons and holes in the non-equilibrium EHP located in the bulk GaAs (the short-wavelength part of the spectrum) and second due to recombination in the

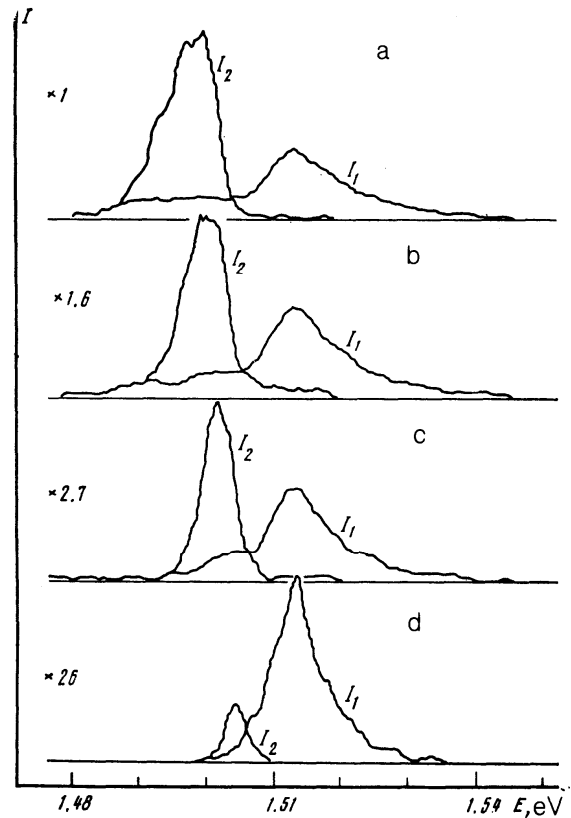


Fig. 2. Spontaneous (I_1) and stimulated (I_2) emission spectra of GaAs- $\text{Al}_{0.3}\text{Ga}_{0.7}\text{As}$ heterostructures at 4.2 K; L in MW/cm^2 equals: 10 (a), 2 (b), 0.8 (c) and 0.04 (d).

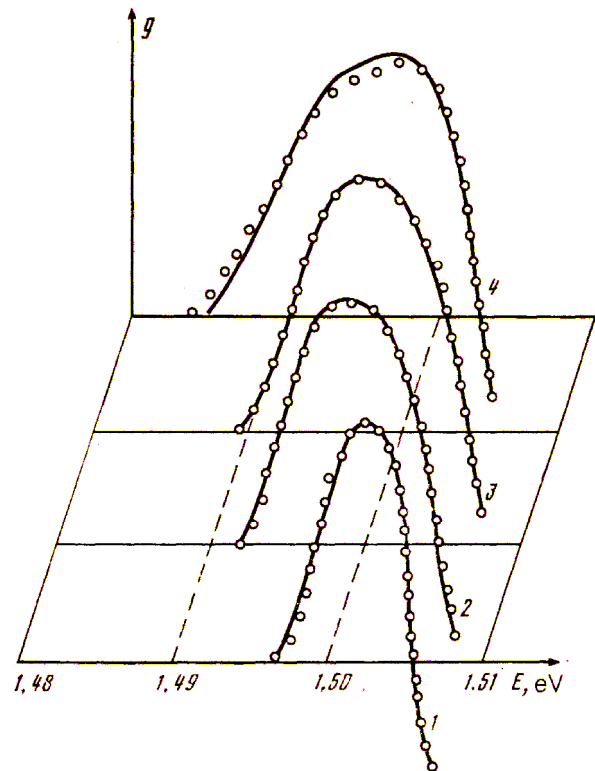


Fig. 3. Optical gain spectra of GaAs- $\text{Al}_{0.3}\text{Ga}_{0.7}\text{As}$ heterostructures for various excitation power densities L ; the points are experimental ($T = 4.2 \text{ K}$), the solid lines are calculated; L in MW/cm^2 is: 0.04 (1), 0.8 (2), 2 (3), 10 (4).

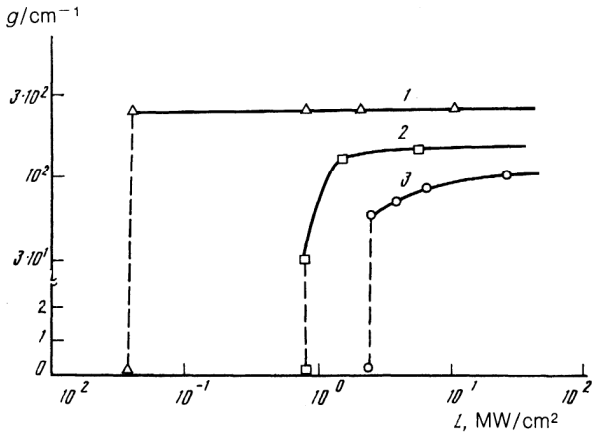


Fig. 4. Dependence of the optical gain coefficient (at its maximum) on the excitation power density for the GaAs-Al_{0.3}Ga_{0.7}As heterostructure (1), the insulator-semiconductor structure Si₃N₄-GaAs (2) and GaAs (3) at 4.2 K.

quasi-2D-EHP localized at the GaAs-Al_{0.3}Ga_{0.7}As boundary (the longwave part of the spectrum). It is noteworthy that stimulated emission was observed in these structures only for the quasi-2D-EHP.

The spectra of the optical gain coefficient g were found from the relation between the stimulated (I_2) and spontaneous (I_1) emission intensities measured at identical pump power densities: $\frac{I_1}{I_2} = \frac{\exp(gl) - 1}{gl}$.

Here, l is the length of that part of the laser beam producing gain (in our case $l = 130 \mu\text{m}$). Fig. 3 presents the calculated spectra of g at four excitation power densities (the points are taken from our experiment). Note the considerable broadening of the optical gain spectrum and its shift toward longer wavelengths with increasing the excitation power density.

Let us consider the optical gain spectrum. Fig. 2 demonstrates that intense stimulated emission is observed only in the spectral region of spontaneous luminescence of 2D-EHP. These results indicate that under conditions that give rise to coexisting of 3D- and 2D-EHP, the optical gain effects take place primarily in 2D-EHP. It is interesting to compare the threshold for appearance of optical gain and the values of g_{max} for 3D- and 2D-EHP. In Fig. 4, we demonstrate the dependence of g_{max} on the excitation power density for the GaAs-Al_{0.3}Ga_{0.7}As heterostructure studied in this paper along with the corresponding dependences [9], for a Si₃N₄-GaAs structure in which quasi-2D-EHP can be obtained, and GaAs with a free surface (with 3D-EHP). The excitation threshold at which optical gain appears in the layered Si₃N₄-GaAs structure is of the factor 3 lower than that of bulk GaAs; for the GaAs-Al_{0.3}Ga_{0.7}As heterostructure, the excitation threshold is lower by the factor 60. At the same time, the maximum value of the optical gain coefficient for the Si₃N₄-GaAs is roughly 1.5 times higher than that in bulk GaAs, while the value for the GaAs-Al_{0.3}Ga_{0.7}As heterostructure is 2.5 times higher. Thus, the transition from 3D-EHP to 2D-EHP significantly decreases the threshold for the appearance of optical gain stimulated beam and simultaneously

increases g . The main physical reason for this is the concentration of plasma along one (normal) coordinate in the 2D case. The obtained results indicate the superiority of 2D-EHP compared with 3D-EHP for designing lasers, which was demonstrated first in [8].

It is clear from the optical gain spectra presented in Fig. 3 for the GaAs-Al_{0.3}Ga_{0.7}As heterostructure that since the level of excitation increases, the spectra broadens, predominantly because of pulling toward the longwave region. We can model this type of behavior by taking into account the so-called “outward streaming effect” in the dynamics of the non-equilibrium carriers; this effect is a consequence of forces acting on the carriers associated with the gradient of the Fermi pressure [6].

A detailed analysis of features of the shape and width of EHL photoluminescence (PL) band dependences both on the temperature (the line narrows with growing the temperature), and on the excitation intensity enabled us to conclude [4, 5] that PL band under consideration is caused by the two-dimensional 2D condensed EHP. A typical feature of this strongly oversaturated EHP (10^{24} quanta/cm²·s) is that the maximum intensity of PL is observed from the edges of the studied samples with the maximum at $\lambda = 829 \text{ nm}$

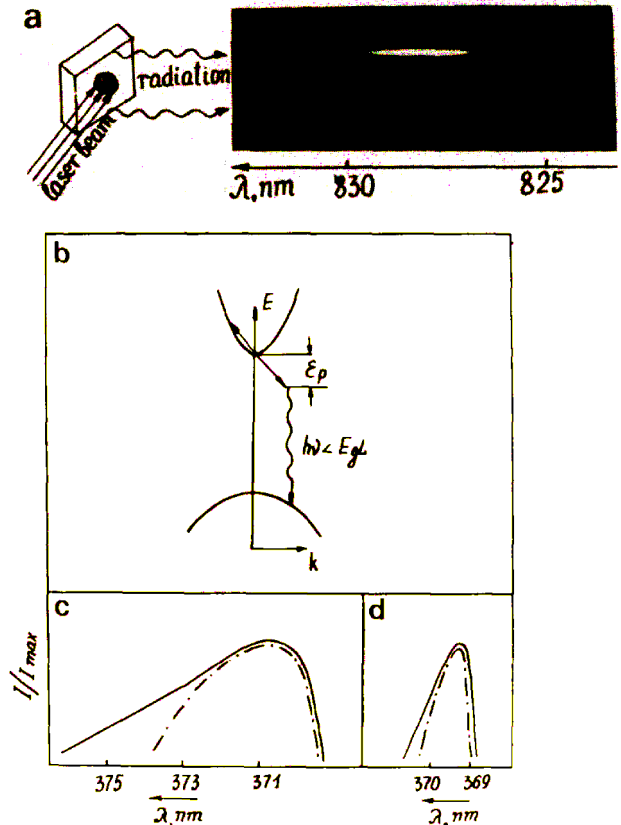


Fig. 5. (a) Spectrogram of the stimulated radiation of GaAs-Si₃N₄ structure, which is excited by a ruby laser. (b) Schematic plot of the three-particle interaction – irradiative recombination of electron-hole pairs with a birth of plasmons. (c), (d) Experimental (solid curves) and theoretical (dash-dotted curves) of the radiation from 3D (c) and quasi-2D (d) EHC, created in ZnO by an optical excitation. $T = 4.2 \text{ K}$.

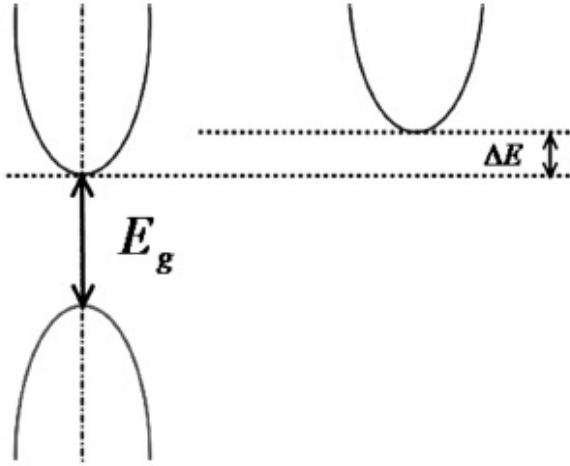


Fig. 6. Structure of the conduction band in monolayers of transition metal chalcogenides. The presence of K - and T -valleys allows the effect of negative differential conductance.

(Fig. 5). This fact proves the appearance of stimulated radiation of EHC amplified by the total internal reflection of the volume resonator formed by the natural crystal planes.

Additional possibilities for obtaining 2D liquid electron-hole plasma at elevated temperatures were analyzed by us in [10]. Thus, for nanostructures ZnO, InP, GaN it is possible to form lasers at elevated temperatures (even higher than the room one) in the case of exciton condensation in quantum-sized structures.

2. Electronic 2D devices based on hot electrons (2D generators – Gunn diodes)

In recent years, various monolayers with semiconducting properties (MoS₂, WSe₂, other chalcogenides of transition metals, black phosphorus, and others; see, *e.g.*, the papers [11, 12]) were intensively synthesized and studied. The most known from this class of materials are the MoS₂ and WS₂ monolayers; these are direct-band semiconductors with the bandgap widths $E_g \approx 1.7$ and 1.8 eV, respectively. The extrema of the conduction and valence bands are located at the points K and K' of the hexagonal Brillouin zone [13], as it also takes place in graphene.

The results of calculations carried out from the first principles, by using the density functional method, demonstrated that the conduction band spectrum of those materials includes a lateral extremum (the T -valley) with energies by approximately 0.2 and 0.08 eV larger than the band bottom energy, which is located in the direction from the points K and K' to the Brillouin zone center Γ (Fig. 6). The energy spectrum near those two extrema is parabolic. The presence of two subbands in the conduction band – lower (denoted by subscript 1) and upper (denoted by subscript 2) ones, for which the effective-mass relation $m_1 < m_2$ for 2D two-dimensional electrons is obeyed [14] – gives us grounds to expect that the effect of negative differential conductance, which is

associated with the filling by field-heated electrons of the higher valley characterized by a higher effective mass, can take place in 2D monolayers of the WS₂ or MoS₂ type [15]. Note that this effect has already been observed in “traditional” (not 2D) quantum heterostructures [16]. Recently, it has been also studied in quantum heterostructures composed of multilayered phosphorus and rhenium disulfide [16] or graphene (ultrathin graphite) and boron nitride [17].

The negative differential conductance has been experimentally revealed quite recently in WS₂ monolayers [18]. It was shown that, if the monolayer is unstrained, the effect does not take place owing to a small energy distance between the valleys, $\Delta E \approx 0.08$ eV, because, at room temperature, electrons begin to fill the T -valley at minimum values of the fields between the gate and drain. However, if a biaxial compression is applied, and $\Delta E \sim 0.1$ eV or somewhat higher, the effect of negative differential conductance begins to be clearly distinguished in the dependence of the current through the field transistor on the field between the gate and drain. The detected effect can open promising prospects for creation of microwave devices in the frequency range of tens of GHz or higher. Therefore, it is important to have a convenient semi-phenomenological model for its description, similarly to that widely used for three-dimensional materials [15]. For the field-heated electrons redistributed between the valleys K (subscript 1) and T (subscript 2), the current density through the semiconductor can be written as follows:

$$J = e(\mu_1 n_1 + \mu_2 n_2) \varepsilon = env, \quad (1)$$

where the electron concentrations $n_{1,2}$ in two subbands are related by the equality $n_1 + n_2 = n$, ε is the electric field, and v – average drift velocity of electrons.

The electron concentration ratio between the subbands is associated with the energy ΔE and temperature of hot electrons T_e by the obvious expression [15]

$$\frac{n_2}{n_1} = R \exp\left(-\frac{\Delta E}{kT_e}\right), \quad (2)$$

where the factor R is the ratio between the numbers of available quantum states in subbands 2 and 1. Taking into account that the degeneration degree equals $g_2 = 2$ in the K -valley, and $g_2 = 6$ in the T -valley [12, 13], and adopting standard expressions for the 2D densities of

state in the case of parabolic spectrum, $D = \frac{g_{1,2} m_{1,2}}{\pi \hbar}$,

$$R = 3 \frac{m_2}{m_1} \gg 1. \quad (3)$$

In the approximation of the energy relaxation time, the dependence of the drift velocity on the field can be written in the standard form

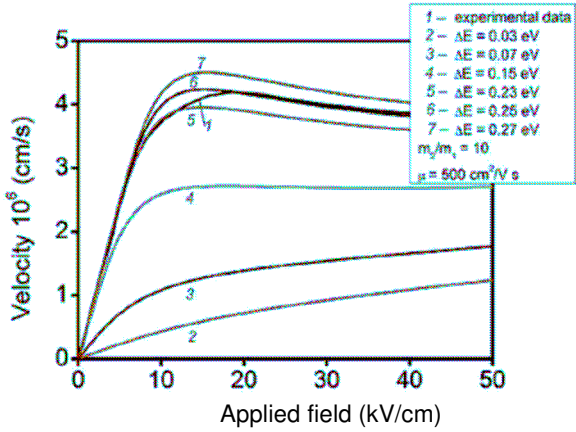


Fig. 7. Dependences of the drift velocity in WS₂ on the applied field calculated according to Eq. (4) for the temperature $T = 300$ K and various ΔE -values.

$$v = \mu_1 \varepsilon \left[1 + \frac{n_2}{n_1} \right]^{-1}. \quad (4)$$

The electron temperature T_e that enters Eqs. (2) and (4) looks like

$$T_e = T + \frac{3e\tau_e\mu_1}{3k} \varepsilon^2 \left[1 + \frac{n_2}{n_1} \right]^{-1}. \quad (5)$$

Fig. 7 demonstrates the dependences of the electron drift velocity (4) in WS₂ on the applied field calculated according to Eqs. (2), (3), and (5) for the temperature $T = 300$ K and various ΔE -values from 0.03 to 0.27 eV.

Fig. 8 exhibits the dependences of the ratio between the electron concentration n_2 in the upper T -valley and the total electron concentration n in the conduction band on the electric field ε calculated for the same room temperature.

In these calculations, the following probable parameter values were used: $\tau_e = 10^{-12}$ s, $\mu_1 = 500$ cm²/(V·s), $m_2/m_1 = 10$. At $\Delta E = 0.25$ eV, the indicated values provide a good agreement with the experimental curve and correlate with the data given for WS₂ in literature. Note that the ratio between the effective masses in the K - and T -valleys (in accordance with the data presented in [18], this parameter equals 0.3 m_0 and 0.75 m_0 , respectively) is somewhat lower, but the given values are relevant only in vicinities of the extrema and do not make allowance for the mass increase with the energy in the T -valley.

One can see from Fig. 7 that, starting from a certain threshold value $\Delta E \approx 0.15$ eV, the dependence $v(\varepsilon)$ acquires a maximum, and the ratio n_2/n begins to grow under the fields corresponding to this maximum (this phenomenon corresponds to the intensive filling the upper valley in the conduction band by heated electrons). At lower ΔE -values, as shown in Fig. 8, electrons actively transit to the upper valley already at the minimum electric field values ε , and the effect of negative differential conductance is absent.

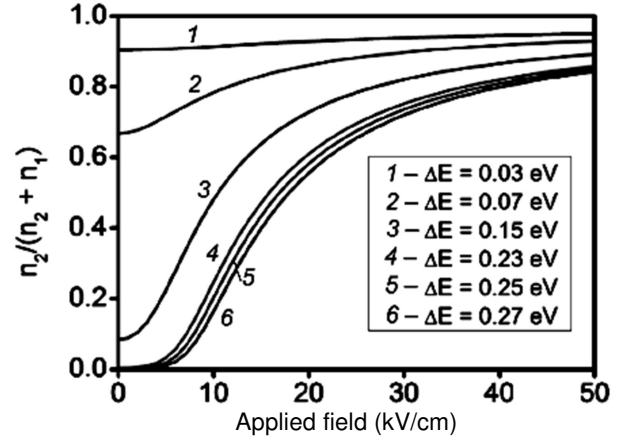


Fig. 8. Dependences of the ratio between the electron concentration in the upper T -valley, n_2 , and the total electron concentration in the conduction band, n , on the electric field calculated for $T = 300$ K.

Hence, the proposed theoretical model of electron heating in the system with two valleys [19], which was adapted by us for the first time to describe 2D semiconductor monolayers of the MoS₂ and WS₂ types, can well describe available experimental data. It confirms the possibility to create a new generation of Gunn diodes on the basis of 2D structures. The frequencies that can be obtained with these diodes can be easily estimated from the relation

$$f \sim \frac{v}{L}, \quad (6)$$

where L is the diode channel length.

For the parameter values corresponding to the system that was studied in [18] ($v = 4 \cdot 10^6$ cm/s and $L = 5$ μm), we obtain $f \sim 10$ GHz, which makes such these potentially attractive for a number of practical applications.

The model described in this paper also makes it possible to estimate a potential capability to create Gunn diodes on the basis of other 2D semiconductor monolayers and thin quantum wells, which are based on both traditional electronic materials and carbon allotropes “between graphene and graphite”. The latter, as we showed in work [20], can also possess useful semiconductor properties.

3. Conclusions

In this review paper, we have discussed two types of 2D structures: 2D atomic layer and 2D electron-hole plasma. 2D layered structures attract the extended interest from the viewpoint to develop new high-tech devices: optical, electrical and others. In a series of papers (see [3-8, 10]) we have demonstrated that 3D electron-hole plasma (3D-EHP) located in the bulk GaAs coexists with 2D-EHP in the GaAs-AlGaAs and GaAs-Si₃N₄ heterostructures. The stimulated emission (necessary condition for creation of

lasers) is predominantly generated in 2D-EHP. The threshold excitation at which optical gain appears in the 2D-EHP is two orders of magnitude lower than in 3D-EHP, while the magnitude of the optical gain coefficient for GaAs-AlGaAs is 2.5 times higher than it is in GaAs under the same photoexcitation conditions. These characteristics are very important in relation with the possible use of a non-equilibrium 2D-EHP as a source of laser light emission.

Other types of 2D structures, for which the theoretical model of electron heating in the system with two valleys was adapted in [19] for the first time to describe 2D semiconductor monolayers of the MoS₂ and WS₂ types, can well describe available experimental data. It confirms the possibility to create a new generation of Gunn diodes on the basis of those structures. The model described in this paper also makes it possible to estimate a potential capability to create Gunn diodes on the basis of other 2D semiconductor monolayers and thin quantum wells, which are based on both traditional electronic materials and carbon allotropes “between graphene and graphite”.

References

1. Rayanov K., Altshuler B.L., Rubo Y.G. and Flach S. Frequency combs with weakly lasing exciton-polariton condensates. *Phys. Rev. Lett.* 2015. **114**. P. 193901. DOI: 10.1103/PhysRevLett.114.193901.
2. Yongzhuo Li, Jianxing Zhang, Dandan Huang, Hao Sun, Fan Fan, Jiabin Feng, Zhen Wang, Ning C.Z. Room-temperature continuous-wave lasing from monolayer molybdenum ditelluride integrated with a silicon nanobeam cavity. *Nature Nanotechnology*. 2017. **12**, No 10. P. 987–992.
3. Zuev V.A., Korbutyak D.V., Litovchenko V.G., Hudymenko L.F. and Hule E.M. Collective effects on semiconductor surfaces (GaAs). *Zh. Eksperim. Teor. Fiz.* 1975. **69**. P. 1289–1300.
4. Zuev V.A., Korbutyak D.V., Kryuchenko Yu.V. and Litovchenko V.G. Electron-hole liquid at the interface of layered structure. *Fiz. Tverd. Tela.* 1978. **20**, Issue 10. P. 2908-2914 (in Russian).
5. Litovchenko V.G., Korbutyak D.V., Kryuchenko Yu.V. Collective properties of excitons in polar semiconductors (ZnO). *Zh. Eksp. Teor. Fiz.* 1982. **81**, Issue 6(12). P. 1965-1976 (in Russian).
6. Litovchenko V.G. Korbutyak D.V. The parameters of quasi-two-dimensional electron-hole plasma stimulated by laser radiation. *Surf. Sci.* 1986. **170**. P. 671–675.
7. Korbutyak D.V. and Litovchenko V.G. Expansion of the electron-hole liquid plasma at GaAs surface. *phys. status solidi (b)*. 1983. **120**, Issue 1. P. 87–97. <https://doi.org/10.1002/pssb.2221200109>.
8. Korbutyak D.V., Kryuchenko Yu.V. and Litovchenko V.G., Baltrameyunas R., Gerazimas E. and Kuokshtis E. Investigation of the optical gain spectra in two-dimensional quantum well heterostructures. *Zh. Eksp. Teor. Fiz.* 1989. **96**. P. 1332–1339.
9. Baltrameyunas R., Gerazimas E., Korbutyak D.V., Kryuchenko Yu.V., Kuokshtis E., Litovchenko V.G. Peculiarities of the optical gain spectra of quasi-two-dimensional electron-hole plasma. *Fiz. Tverd. Tela.* 1988. **30**, Issue 7. P. 2020–2023 (in Russian).
10. Litovchenko V.G., Grygoriev A.A. Electron-hole Fermi liquid in nanosized semiconductor structures. *Semiconductor Physics, Quantum Electronics & Optoelectronics*. 2010. **13**, No 1. P. 051–057.
11. Miró P., Audiffred M., Heine T. An atlas of two-dimensional materials. *Chem. Soc. Rev.* 2014. **43**, No 18. P. 6537.
12. Xinming Li, Li Tao, Zefeng Chen, Hui Fang, Xuesong Li, Xinran Wang, Jian-Bin Xu, and Hongwei Zhu. Graphene and related two-dimensional materials: Structure-property relationships for electronics and optoelectronics. *Appl. Phys. Rev.* 2017. **4**. P. 021306. DOI: 10.1063/1.4983646.
13. Yazyev O.V., Kis A. MoS₂ and semiconductors in the flatland. *Mater. Today*. 2015. **18**. P. 20–30.
14. Jaewoo Shim, Seyong Oh, Dong-Ho Kang, Seo-Hyeon Jo, M.H. Ali, Woo-Young Choi, Keun Heo, Jaeho Jeon, Sungjoo Lee, Minwoo Kim, Young Jae Song, Jin-Hong Park. Phosphorene/rhenium disulfide heterojunction-based negative differential resistance device for multi-valued logic. *Nature Commun.* 2016. **7**. P. 13413. DOI: 10.1038/ncomms13413.
15. Sze S.M. *Physics of Semiconductor Devices*. Wiley, 1981.
16. *Negative Differential Resistance and Instabilities in 2-D Semiconductors*. Ed. by N. Balkan, B.K. Ridley, A.J. Vickers. Plenum Press, 1993.
17. Zhao Y., Wan Z., Hetmaniuk U., Anantram N.P. Negative differential resistance in graphene boron nitride heterostructure controlled by twist and phonon-scattering. ArXiv: 1702.04435 (2017).
18. He G., Nathawat J., Kwan C.-P. et al. Negative differential conductance and hot-carrier avalanching in monolayer WS₂ FETs. *Sci. Rep.* 2017. **7**. P. 11256. <https://doi.org/10.1038/s41598-017-11647-6>.
19. Lytovchenko V.G., Kurchak A.I., Strikha M.V. Theoretical model for negative differential conductance in 2D semiconductor monolayers. *Ukr. J. Phys.* 2018. **63**, No 6. P. 527–530. <https://doi.org/10.15407/ujpe63.6.527>
20. Lytovchenko V., Kurchak A., Strikha M. The semi-empirical tight-binding model for carbon allotropes “between diamond and graphite”. *J. Appl. Phys.* 2014. **115**. P. 243705. <https://doi.org/10.1063/1.4885060>.

Authors and CV



D.V. Korbutyak Doctor of Physical and Mathematical Sciences, Professor, Laureate of the State Prize of Ukraine in the field of science and technology.

The main scientific works are devoted to the study of the luminescence properties of non-doped and doped with various impurities A^2B^6 nanocrystals, hybrid semiconductor-metal nanostructures, and to elucidation of mechanisms of radiative processes in semiconductor nanocrystals. He is the author of two monographs, over 300 scientific works in the area of semiconductor physics and nanocrystals.

Head of the Semiconductor Nanophotonics Department at the V. Lashkaryov Institute of Semiconductor Physics, National Academy of Sciences of Ukraine.

E-mail: kdv45@isp.kiev.ua



V.G. Lytovchenko Doctor of Physical and Mathematical Sciences, Corresponding Member of the National Academy of Sciences of Ukraine, Laureate of the State Prize of Ukraine in the field of science and technology.

He is one of the founders of the direction Surface Physics of Semiconductors and Microelectronics. Discovered a number of new effects (luminescent surface glow, stimulated by defects of the splitting of bands in thin graphite-like films). He is the author of 10 monographs and over 500 scientific papers.

Head of the Department of Physics of the Surface of Semiconductors and Microelectronics at the V. Lashkaryov Institute of Semiconductor Physics, National Academy of Sciences of Ukraine.



M.V. Strikha Doctor of Physical and Mathematical Sciences, Deputy Minister of Education and Science of Ukraine.

He constructed a consistent theory of optical and recombination transitions in semiconductors with defects, deformations, heterogeneities of composition. In recent years, the main scientific interests are related to the physics of graphene.